FUDMA Journal of Sciences (FJS)
ISSN online: 2616-1370
ISSN print: 2645 - 2944
Vol. 4 No. 1, March, 2020, pp 600 –606

THE IMPORTANCE OF FILM THICKNESS ON THE PHOTOVOLTAIC PERFORMANCE OF PEROVSKITE SOLAR CELLS

[*1,2]Sanni, D. M., [2]Joseph, E. and [2]Adamu, M. A.

[1]Department of Theoretical and Applied Physics, African University of Science and Technology (AUST), Abuja, Nigeria
[2]Department of Physics, Federal University Dutsin-Ma, Katsina State, Nigeria

[*]Corresponding author's email: dahirusanni@gmail.com

ABSTRACT

In this study, we investigated the role of film thickness on the photovoltaic performance of perovskite solar cells (PSCs) fabricated from dehydrated lead acetate as the source material. The inverted p-i-n planar heterojunction architecture was adopted in this work. One step spin-coating methods were used in depositing the perovskite solution before annealing on a hot plate at 90 °C for 5 minutes to form the perovskite film. We varied the film thickness by varying the spin-coating rate from 2000 to 6000 rpm for 60 seconds and the optimal film thickness was obtained at 4000 rpm corresponding to 400 nm. This gave the best power conversion efficiency (PCE) of 11.61%, Open circuit voltage (Voc) of 0.909 V, short circuit photocurrent density (Jsc) of 20.41 mA/cm^2 and fill factor (FF) of 62.56%. Our investigations revealed that film thickness has great influence in the photovoltaic performance of PSCs.

Keywords: Film thickness, perovskite solar cells, spin-coating rate

INTRODUCTION

Methylammonium lead halide perovskites are emerging as a unique group of absorbers for efficient perovskite solar cells (PSCs). This is because they display various advantages, such as inherent broad spectral absorption, ambipolar transport properties, long carrier transport diffusion length, tunable bandgap, light weight and facile solution processability (Kim et al., 2012; Lee, Teuscher, Miyasaka, Murakami, & Snaith, 2012; Stranks et al., 2013; Xing et al., 2013). Significant success has been recorded in recent years with power conversion efficiency (PCE) increased from 3.8% in 2009 to the current record of 25.2% (Feldmann et al., 2020; Kojima, Teshima, Shirai, & Miyasaka, 2009). Devices with different structures of Perovskite solar cells have been investigated and reported extensively in recent years which includes perovskite sensitized solar cells (Im, Lee, Lee, Park, & Park, 2011), mesoscopic perovskite solar cells (Q. Chen et al., 2013) and planar heterojunction perovskite solar cells(M. Liu, Johnston, & Snaith, 2013; Ye-Jin et al., 2014; Zhou et al., 2014). The planar heterojunction architecture can either be n-i-p or inverted p-i-n. Both the planar heterojunction and mesoporoues architectures have recorded a high PCE (Etgar et al., 2012; M.-H. Liu et al., 2016; Tan et al., 2017; Zhou et al., 2014). The mesoporous architecture has some limitations in the choice of substrates because of the high processing temperature of over 450 °C (Burschka et al., 2013), which hinders its applications on flexible substrate and normal glass (You, Hong, Yang, Chen, Cai, Song, Chen, et al., 2014). The planar heterojunction architecture, on the other hand, is compatible with a flexible substrate (polymer) because of its low processing temperature below 100 °C (Docampo, Ball, Darwich, Eperon, & Snaith, 2013; You, Hong, Yang, Chen, Cai, Song, & Chen, 2014). Besides the choice of the polymer substrate, the low processing temperature of the planar heterojunction architecture gives the advantages of choosing a wide range of electrodes and functional layers such as organic holes transport layers (PEDOT:PSS) and organic electron transport layers (PCBM) (You, Hong, Yang, Chen, Cai, Song, Chen, et al., 2014).

Different methods have been used in depositing perovskite films such as dip-coating, spray coating, vapor deposition, vapor-assisted solution deposition, one-step spin coating process, and two-step sequential deposition (Burschka et al., 2013; Q. Chen et al., 2014; Docampo et al., 2013; Heo et al., 2013; Kim et al., 2012). The one-step spin coating and the two steps spin coating are the most widely used methods for depositing perovskite films, which are solution-processed and requires thermal or solvent annealing, hence they are cost-effective methods of producing perovskite films and these methods also allow mass production for commercial purposes.

Perovskite $CH_3NH_3PbI_3$ films are usually produced by the reaction of CH_3NH_3I and PbI_2 in ratio 1:1 solution as shown in equation (1). Attempts have also been made in synthesizing $CH_3NH_3PbI_3$ films from non-halides Pb precursors like lead acetate ($Pb(OAc)_2$), lead nitrate $Pb(NO_3)$, Lead (II) acetylacetonate $(Pb(acac)_2$ and lead (II) carbonate ($PbCO_3$) (Aldibaja, Fadi Kamal Badia, Laura Mas-Marzá, Elena Sánchez, Rafael S. Barea, Eva M. Mora-Sero, 2015; Andrei Buin, Patrick Pietsch, Oleksandr Voznyy & Comin, Alexander H Ip, Edward H. Sargent, 2014; Y. Chen, Yerramilli, Shen, Zhao, & Alford, 2018; Li et al., 2016; Moore, Sai, Tan, Estroff,

& Wiesner, 2014; Qing et al., 2015; Sanni et al., 2019; Sima, Vasile, & Sima, 2017; Yerramilli et al., 2018) with $Pb(OAc)_2$ been the most successful of the non-halide Pb precursor based PSCs. The equation for the reaction of lead acetate as source material is presented in equation (2) (Zhang et al., 2015). The reaction in equation (2) gives rise to the perovskite film $CH_3NH_3PbI_3$ and the byproduct N-methylammonium acetate $2CH_3NH_3COO$ which will be evaporated during thermal or solvent annealing.

$$PbI_2 + CH_3NH_3I \rightarrow CH_3NH_3PbI_3 \quad (1)$$

$$Pb(CH_3OO)_2 + 3CH_3NH_3I \rightarrow CH_3NH_3PbI_3 + 2CH_3NH_3COO \uparrow \quad (2)$$

In this research, the one-step spin-coating method was used to investigate the role of film thickness on the photovoltaic performance of PSCs. In the spin-coating technique the thickness of the film depends on the spin coating rate (speed). We fabricated five different devices with different spin-coating rate of 2000, 3000, 4000, 5000 and 6000 rpm respectively and denoted the devices as A, B, C, D and E respectively. A power conversion efficiency (PCE) of 11.61% was obtained with a spin-coating rate of 4000 rpm.

EXPERIMENTAL

MATERIALS

Lead acetate trihydrate ($PbAc_2.3H_2O$) was purchased from Alfa Aesar, while methylammonium iodide (MAI) was supplied by Ossila. ($PbAc_2.3H_2O$) was processed further under a flowing nitrogen gas at 79°C to obtained the dehydrated lead acetate ($Pb(Ac)_2$. Poly (3,4-ethylene dioxythiophene): poly (styrene sulfonate) (PEDOT:PSS) was obtained from Ossila. The precursor was prepared by dissolving 3.0 mmol MAI and 1.0 mmol $Pb(Ac)_2$ in 1mL dimethylformamide (DMF) solvent.

DEVICE FABRICATION

The devices structure was ITO/PEDOT:PSS/$CH_3NH_3PbI_3$/PCBM/Ag. The pre-patterned glass/indium tin oxide (ITO) substrates were sequentially cleaned in a detergent solution, deionized water, acetone and isopropyl alcohol (IPA) in an ultrasonic bath for 15 munites an hour. Finally, they were treated by exposing them to ultraviolet-ozone (UVO) for 15 minutes to get rid of any remaining impurity. The hole transport layer of PEDOT:PSS, was filtered through a 0.45 μm filter and the filtered solution was spin-coated onto the patterned ITO substrates at a spin-coating rate of 4000 rpm for 60 secs before annealing at 135 °C for 15 minutes. The solutions of MAI:$Pb(Ac)_2$ were then spin-coated on the PEDOT:PSS layer at the rate of 2000, 3000, 4000, 5000 and 6000 rpm for 60 secs (the corresponding devices are denoted as A, B, C, D and E) respectively before they were thermal anneal on the hot plate at the temperatures of 90 °C for 5 minutes. These processes resulted in perovskite films.

After that, the electron collection layer of phenyl-C_{61}-butyric acid methyl ester (PCBM, Ossila) was obtained by dissolving the solutes into a chlorobenzene solvent (20 mg/mL) and spin-coating it on $CH_3NH_3PbI_3$ layer at the rate of 1000 rpm for 30 s. Lastly, the silver (Ag) electrode was deposited on the PCBM to complete the device fabrication process. The fabricated device is an inverted planar heterojunction solar cell (see Fig. 2(d)). The dimension of the substrate is 2.5 cm × 2.5 cm and the active area is 0.2 cm^2

DEVICE CHARACTERIZATION

The current density-voltage (J-V) measurements of the solar cells devices were observed on a Keithley 2400, under simulated AM1.5G irradiation (100 mW/cm^2) with a Xenon-lamp-based solar simulator (Spectra Physics, Oriel Instruments, USA)

RESULTS AND DISCUSSIONS

The device structure employed in this research to investigate the influence of perovskite film thickness on the photovoltaic properties is the inverted planar heterojunction architecture p-i-n as shown in Fig. 2(d). $Pb(Ac)_2$ is used as the Pb source with MAI to obtain the perovskite film ($CH_3NH_3PbI_3$) as stated in equation (2). The total PCE of solar cells depends on the open-circuit voltage (Voc), the short circuit photocurrent density (Jsc), the fill factor (FF) and the intensity of the incident light (Pin) as represented in equation (3) (Yoshida et al., 1997). The J-V curve showing the photovoltaic performance of the perovskite solar cells derived from different perovskite film thickness is shown in Fig. 1(a-f) and (table 1) shows the device parameters.

$$\text{PCE} = \frac{J_{sc}V_{oc}FF}{P_{in}} \quad (3)$$

From the J-V curve in Fig. 1 and the summary of the photovoltaic properties in table 1 it is noted that device C fabricated with a spin-coating rate of 4000 rpm for 60 seconds has the best performing PCE of 11.61%, Voc of 0.909 V, Jsc of 20.41 mA/cm^2 and FF of 62.56%, while devices A and E have the lowest PCE of 5.81% and 5.84% respectively. The reason for the low PCE of device A could be due to the poor perovskite film formation due to the low rate of deposition of 2000 rpm. At this rate, the film formation is not uniform resulting in some portion of the film to be too thick and some portion to be too thin. This poor film formation resulted in low Voc and by implication low PCE as it is observed in Fig. 1(a). On the other hand, the reason for the low PCE of device E is because at 6000 rmp the film becomes too thin which limits the amount of solar energy that can be absorbed by the photoactive layer which is evident in the low Jsc of device E as shown in Fig 1(e).

The main reason for the increase of *PCE* of device *C* is an increase of *Jsc*. The higher Jsc of a device is attributed to a smoother surface and better crystallinity of perovskite films.
The increase of Jsc for device C seems to be a major effect from free charge- (carrier density (n) for good quality perovskite films according to a recombination dynamic relation Wang, Chen, Han, Zhang, & Ma, 2016)

$$\frac{dn(t)}{dt} = -k_3 n^3 - k_2 n^2 - k_1 n^1 \qquad (4),$$

where k_1, k_2 and k_3 are trap-assisted recombination rate, radiative recombination rate and Auger recombination rate, respectively. In this case, good quality films could be considered to reduce the trap-assisted recombination rate. When charge transfers through poor films, some of them might be trapped at the defect site and recombined to decrease Jsc. On the other hand, good films will contribute to better charge transfer with lower trapped state increasing of *Jsc* as seen in Table 1. The trapped state can affect the performance of perovskite solar cells by reducing *Jsc* due to the slow movement of electrons which inturns increase the recombination effect.

To further understand the influence of film thickness on the photovoltaic performance of PSCs, a semi-logarithmic plots of the dark J−V characteristics shown in Fig. 2(a) was employed. From the semi-log plots it is observed that devices A and E have the highest leakage current while devices C and D have the lowest leakage current. The high leakage current in devices A and E could signifies that the electrons are not well extracted from the photoactive layer. On the other hand, the decreased leakage current in devices C and D could be that the electron transport layer are effectively extracted from the perovskite layer.
The abnormal hysteresis in the J-V curves has shown to be a major challenge in evaluating perovskite solar cells (Shao, Xiao, Bi, Yuan, & Huang, 2014). In this research, we studied the hysteresis of device C to be certain of the accuracy of the measurement. We measure the forward and the reverse scan of the J-V curve of the champion cell as presented in Fig. 2(b) which shows that there is no hysteresis observe. The efficiency box plot from 15 devices shown in Fig. 2(c) indicates that the device C performed better statistically compared to devices derived from other film thickness. Devices A, B and C show better repeatability compared to devices D and E this is because there are fewer pin-holes in the perovskite films due to their relative film thickness.

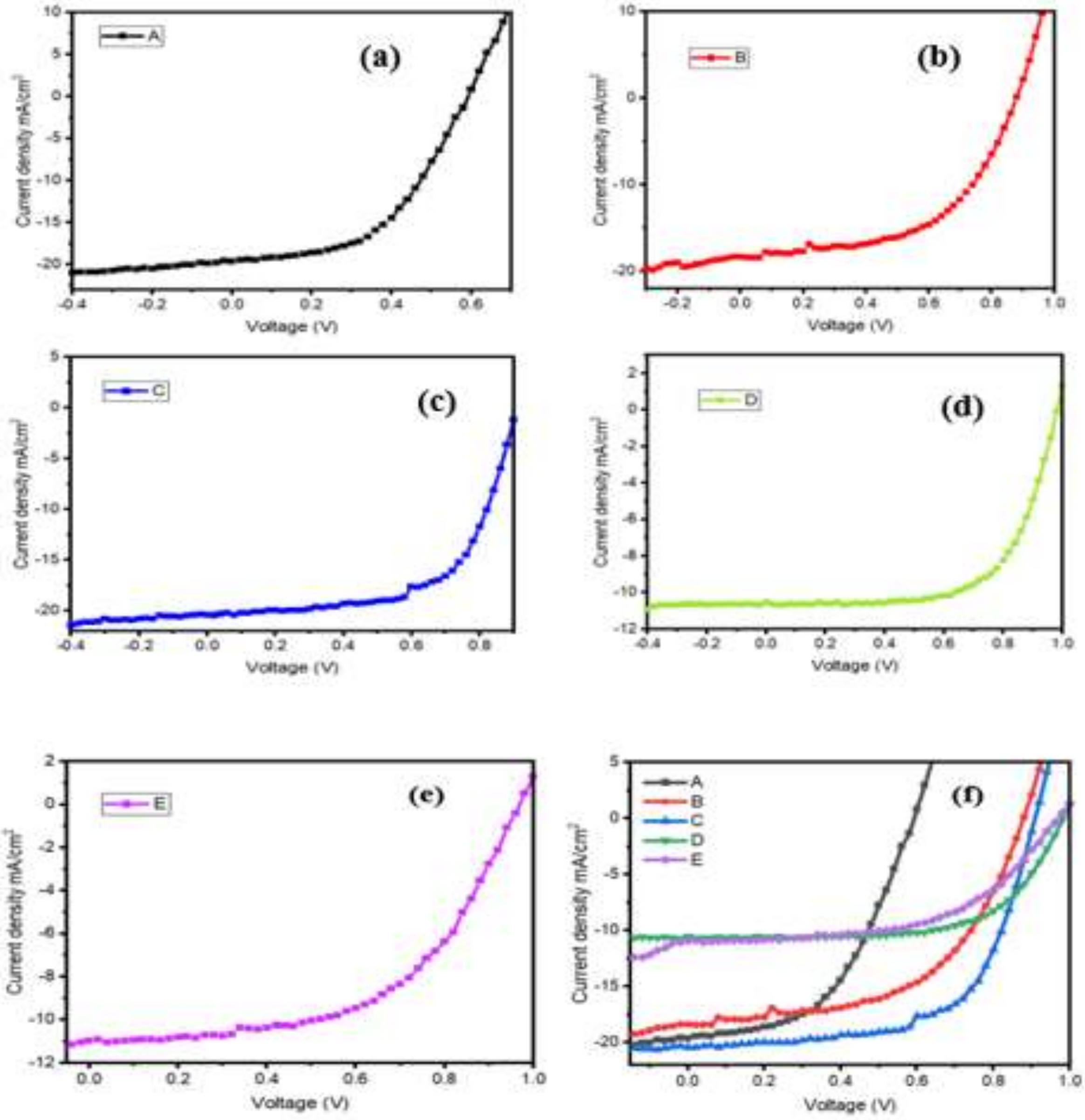

Fig. 1: J-V curves of devices derived from different spin-coating rate (a) 2000 rpm (b) 3000 rpm (c) 4000 rpm (d) 5000, (e) 6000 rpm and (f) J-V curve for the combined devices a-e

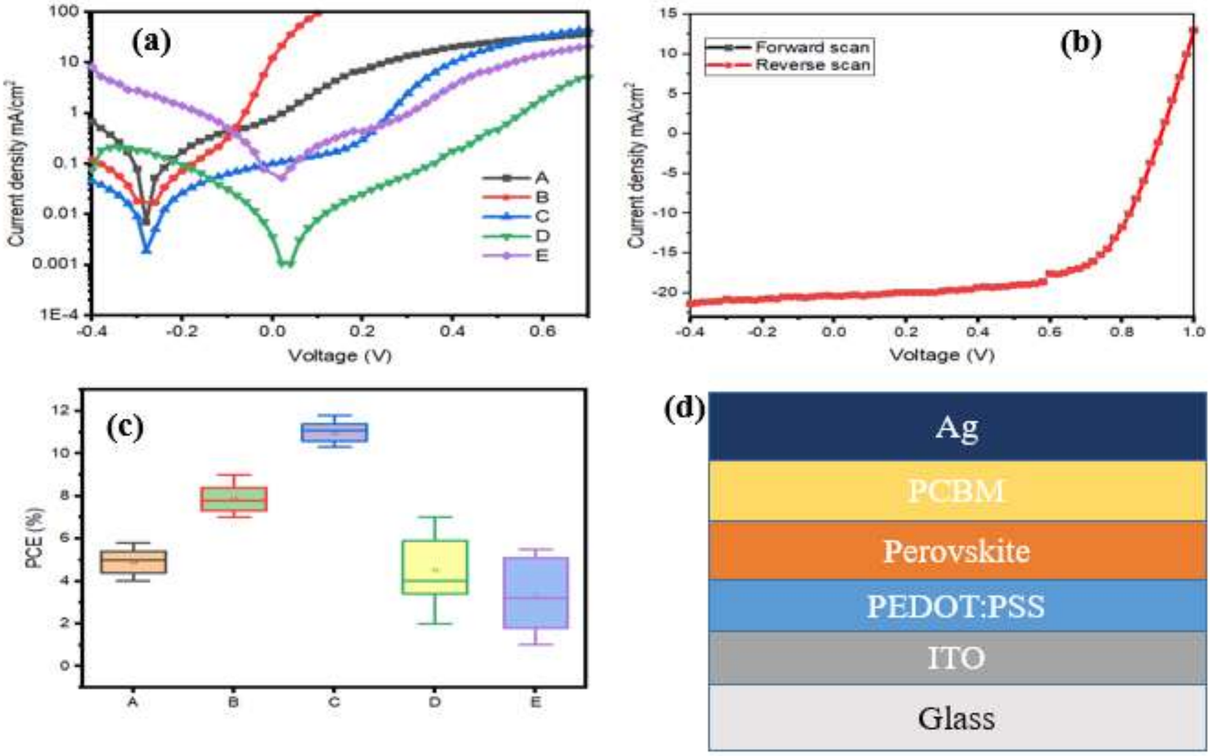

Fig. 2: (a) The semi-logarithmic plots of dark J−V characteristics for the inverted planner perovskite solar cells derived with different spin-coating rate (b) Forward and reverse J-V curves of the champion cell with a spin-coating rate of 4000 rpm (c) Box plot of 15 devices with different deposition rate (d) Schematic diagram of the inverted planar heterojunction perovskite solar cell architecture

Table 1: **Photovoltaic properties for the inverted planar perovskite solar cells with different spin-coating rate**

Devices	V_{oc} (V)	J_{sc} (mA/cm^2)	FF (%)	PCE (%)
A	0.593	19.65	49.87	5.81
B	0.879	18.38	54.46	8.80
C	0.909	20.41	62.56	11.61
D	0.982	10.56	65.63	6.80
E	0.969	10.96	54.96	5.84

CONCLUSION

We used one step spin-coating method to investigate the impact of film thickness on the photovoltaic performance of PSCs. The investigation reveals that film thickness has great effect on the performance and production of PSCs. Device C which was fabricated with a spin-coating rate of 4000 rpm for 60 seconds and a corresponding film thickness of 400 nm produce the best PCE of 11.61% while the lowest PCE is produced by device E which was fabricated with spin-coating speed of 6000 rpm and with a corresponding film thickness of 250 nm.

ACKNOWLEDGMENT

This study was sponsored by Pan African Materials Institute (AUST/PAMI/2015 5415-NG) through funding from the World Bank African Centers of Excellence Program to whom the authors are greatly indebted

REFERENCES

Aldibaja, Fadi Kamal Badia, Laura Mas-Marzá, Elena Sánchez, Rafael S. Barea, Eva M. Mora-Sero, I. (2015). Effect of different lead precursors on perovskite solar cell performance and stability. *J. Mater. Chem. A*, *3*(17), 9194–9200. https://doi.org/10.1039/C4TA06198E

Andrei Buin, Patrick Pietsch, Oleksandr Voznyy, R., & Comin, Alexander H Ip, Edward H. Sargent, and B. X. (2014). Materials Processing Routes to Trap-free Halide Perovskites. *Nano Letters*, 1–24. https://doi.org/10.1021/nl502612m

Burschka, J., Pellet, N., Moon, S. J., Humphry-Baker, R., Gao, P., Nazeeruddin, M. K., & Grätzel, M. (2013). Sequential deposition as a route to high-performance perovskite-sensitized solar cells. *Research Letter*, 1–5. https://doi.org/10.1038/nature12340

Chen, Q., Zhou, H., Hong, Z., Luo, S., Duan, H.-S., Wang, H.-H., … Yang, Y. (2013). Planar heterojunction perovskite solar cells via vapor-assisted solution process. *Journal of the American Chemical Society*, *136*(2), 622–625.

Chen, Q., Zhou, H., Hong, Z., Luo, S., Duan, H., Wang, H., … Yang, Y. (2014). Planar Heterojunction Perovskite Solar Cells via Vapor-Assisted Solution Process. *Journal of the American Chemical Society*, *136(2)*(Scheme 1), 3–6. https://doi.org/10.1021/ja411509g

Chen, Y., Yerramilli, A., Shen, Y., Zhao, Z., & Alford, T. (2018). Effect of excessive Pb content in the precursor solutions on the properties of the lead acetate derived CH3NH3PbI3 perovskite solar cells. *Solar Energy Materials and Solar Cells*, *174*(June 2017), 478–484. https://doi.org/10.1016/j.solmat.2017.09.039

Docampo, P., Ball, J. M., Darwich, M., Eperon, G. E., & Snaith, H. J. (2013). Efficient organometal trihalide perovskite planar-heterojunction solar cells on flexible polymer substrates. *Nature Communications*, *4file:///C*, 1–6. https://doi.org/10.1038/ncomms3761

Etgar, L., Gao, P., Xue, Z., Peng, Q., Chandiran, A. K., & Liu, B. (2012). Mesoscopic CH3NH3PbI3 /TiO2 Heterojunction Solar Cells, 8–11. https://doi.org/10.1021/ja307789s

Feldmann, S., Macpherson, S., Senanayak, S. P., Abdi-jalebi, M., Rivett, J. P. H., Nan, G., … Deschler, F. (2020). Photodoping through local charge carrier accumulation in alloyed hybrid perovskites for highly efficient luminescence. *Nature Photonics*, *14*, 123–128.

Heo, J. H., Im, S. H., Noh, J. H., Mandal, T. N., Lim, C. S., Chang, J. A., … Seok, S. Il. (2013). Efficient inorganic-organic hybrid heterojunction solar cells containing perovskite compound and polymeric hole conductors. *Nature Photonics*, *7*(6), 1–6. https://doi.org/10.1038/nphoton.2013.80

Im, J.-H., Lee, C.-R., Lee, J.-W., Park, S.-W., & Park, N.-G. (2011). 6.5% Efficient Perovskite Quantum-Dot-Sensitized Solar Cell. *Nanoscale*, *3*(10), 4088–4093. https://doi.org/10.1039/c1nr10867k

Kim, H.-S., Lee, C.-R., Im, J.-H., Lee, K.-B., Moehl, T., Marchioro, A., … Park, N.-G. (2012). Lead Iodide Perovskite Sensitized All-Solid-State Submicron Thin Film Mesoscopic Solar Cell with Efficiency Exceeding 9%. *SCIENTIFIC REPORTS*, *2:591*, 1–7. https://doi.org/10.1038/srep00591

Kojima, A., Teshima, K., Shirai, Y., & Miyasaka, T. (2009). Organometal halide perovskites as visible-light sensitizers for photovoltaic cells. *Journal of the American Chemical Society*, *131*(17), 6050–6051. https://doi.org/10.1021/ja809598r

Lee, M. M., Teuscher, J., Miyasaka, T., Murakami, T. N., & Snaith, H. J. (2012). Efficient Hybrid Solar Cells Based on Meso-Superstructured Organometal Halide Perovskites. *Reports*, *338*(November), 643–648. https://doi.org/10.1126/science.1228604

Li, C., Guo, Q., Qiao, W., Chen, Q., Ma, S., Pan, X., … Tan, Z. (2016). Efficient lead acetate sourced planar heterojunction perovskite solar cells with enhanced substrate coverage via one-step spin-coating. *Organic Electronics: Physics, Materials, Applications*, *33*, 194–200. https://doi.org/10.1016/j.orgel.2016.03.017

Liu, M.-H., Zhou, Z.-J., Zhang, P.-P., Tian, Q.-W., Zhou, W.-H., Kou, D.-X., & Wu, S.-X. (2016). p-type Li, Cu-codoped NiOx hole-transporting layer for efficient planar perovskite solar cells. *Optics Express*, *24*(22), 128–132. https://doi.org/org/10.1364/OE.24.0A1349

Liu, M., Johnston, M. B., & Snaith, H. J. (2013). Efficient planar heterojunction perovskite solar cells by vapour deposition. *Nature*, *501*(7467), 395–398. https://doi.org/10.1038/nature12509

Moore, D. T., Sai, H., Tan, K. W., Estroff, L. A., & Wiesner, U. (2014). Impact of the organic halide salt on final perovskite composition for photovoltaic applications composition for photovoltaic applications. *APL Materials*, *2*(May). https://doi.org/10.1063/1.4886275

Qing, J., Chandran, H. T., Xue, H. T., Guan, Z. Q., Liu, T. L., Tsang, S. W., … Lee, C. S. (2015). Simple fabrication of perovskite solar cells using lead acetate as lead source at low temperature. *Organic Electronics: Physics, Materials, Applications*, *27*, 12–17. https://doi.org/10.1016/j.orgel.2015.08.021

Sanni, D. M., Chen, Y., Yerramilli, A. S., Ntsoenzok, E., Asare, J., Adeniji, S. A., … Alford, T. L. (2019). An approach to optimize pre ‐ annealing aging and anneal conditions to improve photovoltaic performance of perovskite solar cells. *Materials for Renewable and Sustainable Energy*, *3*, 1–10. https://doi.org/10.1007/s40243-018-0139-3

Shao, Y., Xiao, Z., Bi, C., Yuan, Y., & Huang, J. (2014). Origin and elimination of photocurrent hysteresis by fullerene passivation in CH3NH3PbI3 planar heterojunction solar cells. *Nature Communications*, *5*, 1–7. https://doi.org/10.1038/ncomms6784

Sima, M., Vasile, E., & Sima, M. (2017). Lead acetate film as precursor for two-step deposition of CH 3 NH 3 PbI 3. *Materials Research Bulletin*, *89*, 89–96. https://doi.org/10.1016/j.materresbull.2017.01.031

Stranks, S. D., Eperon, G. E., Grancini, G., Menelaou, C., Alcocer, M. J. P., Leijtens, T., … Snaith, H. J. (2013). Electron-Hole Diffusion Lengths Exceeding 1 Micrometer in an Organometal Trihalide Perovskite Absorber. *Reports*, *342*(October), 341–345. https://doi.org/10.1126/science.1243982

Tan, H., Jain, A., Voznyy, O., Lan, X., De Arquer, F. P. G., Fan, J. Z., … Sargent, E. H. (2017). Efficient and stable solution-processed planar perovskite solar cells via contact passivation. *Science*, *355*(6326), 722–726. https://doi.org/10.1126/science.aai9081

Xing, G., Mathews, N., Lim, S. S., Lam, Y. M., Mhaisalkar, S., & Sum, T. C. (2013). Long-Range Balanced Electron- and Hole-Transport Lengths in Organic-Inorganic CH3NH3PbI3. *Science*, *342*(October), 344–348. https://doi.org/10.1126/science.1243167

Ye-Jin, J., Lee, S., Kang, R., Kim, J.-E., Yeo, J.-S., Lee, S.-H., … Kim, D.-Y. (2014). Planar heterojunction perovskite solar cells with superior reproducibility. *Scientific Reports*, *4*, 1–7. https://doi.org/10.1038/srep06953

Yerramilli, A. S., Chen, Y., Sanni, D., Asare, J., Theodore, N. D., & Alford, T. L. (2018). Impact of excess lead on the stability and photo-induced degradation of lead halide perovskite solar cells. *Organic Electronics: Physics, Materials, Applications*, *59*. https://doi.org/10.1016/j.orgel.2018.04.052

Yoshida, T., Fujikake, S., Kato, S., Tanda, M., Tabuchi, K., Takano, A., … Sakai, H. (1997). Development of process technologies for plastic-film substrate solar cells. *Solar Energy Materials and Solar Cells*, *48*, 383–391. https://doi.org/org/10.1016/S0927-0248(97)00167-0

You, J., Hong, Z., Yang, Y. (Michael), Chen, Q., Cai, M., Song, T.-B., … Yang, Y. (2014). Low-Temperature Solution-Processed Perovskite Solar Cells with High Efficiency and Flexibility, (Xx). https://doi.org/10.1021/nn406020d

You, J., Hong, Z., Yang, Y. M., Chen, Q., Cai, M., Song, T., & Chen, C. (2014). Perovskite Solar Cells with High Effi ciency and Flexibility, (2), 1674–1680. https://doi.org/10.1021/nn406020d

Zhang, W., Saliba, M., Moore, D. T., Pathak, S. K., Hörantner, M. T., Stergiopoulos, T., … Snaith, H. J. (2015). Ultrasmooth organic-inorganic perovskite thin-film formation and crystallization for efficient planar heterojunction solar cells. *Nature Communications*, *6*, 1–10. https://doi.org/10.1038/ncomms7142

Zhou, H., Chen, Q., Li, G., Luo, S., Song, T., Duan, H.-S., … Yang, Y. (2014). Interface engineering of highly efficient perovskite solar cells. *Reseach Reports*, *345*(6196), 542–546. https://doi.org/10.1126/science.1254050